

Design and characterization of GaN/InGaN solar cells

Omkar Jani^{a)} and Ian Ferguson

School of Electrical and Computer Engineering, Georgia Institute of Technology, Atlanta, Georgia 30332, USA

Christiana Honsberg

Department of Electrical and Computer Engineering, University of Delaware, Newark, Delaware 19716, USA

Sarah Kurtz

National Renewable Energy Laboratory, Golden, Colorado 80401, USA

(Received 22 July 2007; accepted 11 September 2007; published online 28 September 2007)

We experimentally demonstrate the III-V nitrides as a high-performance photovoltaic material with open-circuit voltages up to 2.4 V and internal quantum efficiencies as high as 60%. GaN and high-band gap InGaN solar cells are designed by modifying PC1D software, grown by standard commercial metal-organic chemical vapor deposition, fabricated into devices of variable sizes and contact configurations, and characterized for material quality and performance. The material is primarily characterized by x-ray diffraction and photoluminescence to understand the implications of crystalline imperfections on photovoltaic performance. Two major challenges facing the III-V nitride photovoltaic technology are phase separation within the material and high-contact resistances. © 2007 American Institute of Physics. [DOI: 10.1063/1.2793180]

The III-V nitride material system, which includes AlN, GaN, InN, and their alloys, has been extensively investigated due to their applications in light-emitting diodes (LEDs), laser diodes, and photodetectors.¹ With the recent revision of the band gap of InN at ~ 0.65 eV,^{2–4} the band gap of the InGaN material system now ranges from the infrared to the ultraviolet region. This direct and wide band gap range makes the InGaN material system useful for photovoltaic applications due to the possibility of fabricating not only high-efficiency multijunction solar cells but also third-generation⁵ devices such as intermediate-band solar cells⁶ based solely on the nitride material system. While the maximum reported efficiency for a solar cell is 39% at 236 suns,⁷ achieved by a triple-junction GaInP–GaInAs–Ge tandem, such devices are approaching maturity in terms of efficiency limits.⁸ Detailed balance modeling indicate that in order to achieve practical terrestrial photovoltaic efficiencies of greater than 50%, materials with band gaps greater than 2.4 eV are required.⁹ In addition to the wide band gap range, the nitrides also demonstrate favorable photovoltaic properties such as low effective mass of carriers, high mobilities, high peak and saturation velocities, high absorption coefficients, and radiation tolerance.¹⁰ The III-V nitride technology has demonstrated the ability to grow high-quality crystalline structures and fabricate optoelectronic devices, which confirms its potential in high-efficiency photovoltaics.

While the commercially available violet and blue LEDs use high-band gap InGaN as the active material, the relevant material for photovoltaics is the lower band gap InGaN employed in recently emerging blue-green LEDs. However, due to the present technological challenges in the epitaxy of low band gap optoelectronic quality InGaN and additional requirements posed during solar cell fabrication, III-V nitride photovoltaics still remain a promising but a largely unexplored application.

The present work demonstrates III-V nitride materials and nitride solar cells for efficient photogeneration as well as simultaneous carrier collection. The schematic of a typically fabricated solar cell with details of its epitaxy is shown in Fig. 1. Undoped lower band gap test InGaN is sandwiched between the top *p*- and the supporting *n*-type GaN junctions to ensure fabrication due to the ease of growth and maturity of fabrication technology for GaN compared to InGaN.

Initial spectrometry of the grown GaN and high-band gap InGaN samples concur with literature values measuring absorption coefficients in the order of 10^5 cm⁻¹ at the band edge¹¹ at 3.2 eV (387 nm). These high values indicate that more than 99% of the incident light with energy greater than the band gap is absorbed within the first 500 nm of the material, limiting the thickness requirement of the solar cell to this value. To maximize absorption in the field bearing *i*-region of a *p-i-n* solar cell for maximum collection, the thickness of the top *p*-region is limited to 100 nm, which is just enough to provide charge for the junction and the top-

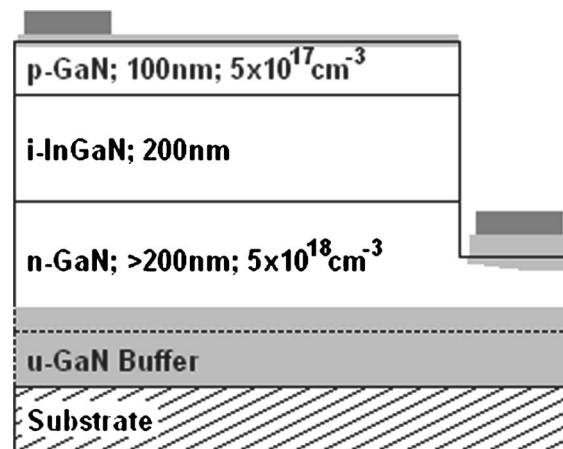


FIG. 1. Structure of typical fabricated GaN/InGaN *p-i-n* solar cells.

^{a)}Electronic mail: jani@ece.gatech.edu

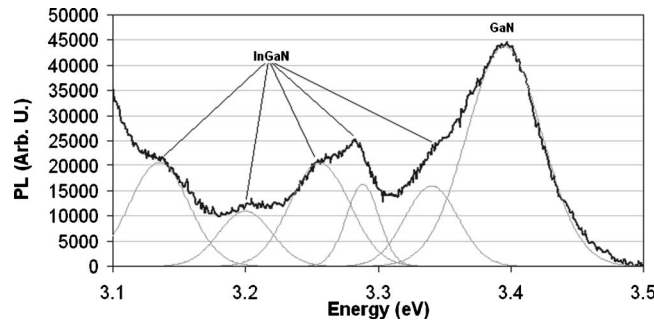


FIG. 2. RT photoluminescence of a typical GaN/InGaN solar cell epitaxial layer grown by MOCVD indicating an evident InGaN phase separation.

metal contacts. The electric field in intrinsic layers of the III-V nitrides decay rapidly with increasing thicknesses due to an unintentional n -type background concentration of 10^{16} cm^{-3} arising from a high defect density in the material. PC1D (Ref. 12) modeling of the energy bands indicates that the i -region maintains a strong electric field of $\sim 40 \text{ kV/cm}$ until a distance of 200 nm from the p -region interface doped at $5 \times 10^{17} \text{ cm}^{-3}$. Hence, the thickness of the i -region is limited to 200 nm. Typical hole diffusion lengths in n -type samples grown previously in the laboratory measure around 200 nm. Hence, the thickness of the n -type layers is designed to be 200 nm.

The epitaxial growth is performed in an Emcore metal-organic chemical vapor deposition (MOCVD) D-125 rotating disk reactor with a short jar configuration. The devices are grown on $2 \mu\text{m}$ GaN nucleation layers over standard 2 in. sapphire substrates. $\text{In}_{0.04}\text{Ga}_{0.96}\text{N}$ and $\text{In}_{0.05}\text{Ga}_{0.95}\text{N}$, with band gaps around 3.2 eV, are used in the i regions of these p - i - n devices. The solar cells are fabricated into 1×1 , 3×3 , and $5 \times 5 \text{ mm}^2$ mesa devices with two primary types of contacting schemes. The initial contacting scheme consists of interdigitated p - and n -contact grids analogous to contacts found in interdigitated back contact solar cells.¹³ A typical finger width is $1 \mu\text{m}$, while the finger spacings used are 50 and $100 \mu\text{m}$. The second contacting scheme is similar to that used in commercial III-V nitride LED technology, which uses a thin Ni–Au semitransparent current spreading layer on the entire top p -type material surface. While this is a mature fabrication method that minimizes series resistance losses in devices, the top-metal layer shades and absorbs a substantial fraction of the incident light as well as enhances front surface recombination.

The epitaxial structures are tested for crystalline perfection by x-ray diffraction using an X'Pert materials research diffractometer (Philips), a high-resolution diffractometer. Typical rocking curves for the $\text{In}_{0.05}\text{Ga}_{0.95}\text{N}/\text{GaN}$ solar cell epilayers measure full widths at half maximum for GaN (peak: 17.28°) at 24.5 arc sec and $\text{In}_{0.05}\text{Ga}_{0.95}\text{N}$ (peak: $\sim 17.19^\circ$) at 72.1 arc sec confirming a high crystalline quality. Optical characterization using room-temperature (RT) photoluminescence reveals phase separation¹⁴ within the material, as shown in Fig. 2. Each Gaussian curve in this figure indicates a separate InGaN phase with band gap corresponding to the center of that curve.

A typical current-voltage (I - V) curve of a solar cell fabricated with grid contacts is shown in Fig. 3(a). The light source used here is modified from a typical one-sun spectrum by increasing its UV content to amplify the response of the solar cell. While the dark curve shows a knee voltage of

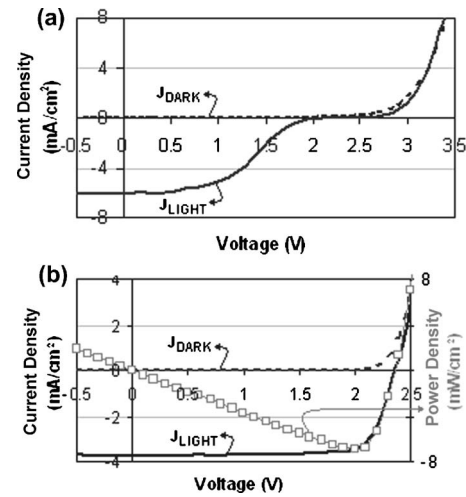


FIG. 3. (a) Typical I - V curve for a GaN/InGaN solar cell with interdigitated grid contacts showing a sharp decrease in the photocurrent before the device reaches open circuit conditions. (b) Typical I - V curve for a GaN/InGaN solar cell with semitransparent current spreading p -contact metal.

3.2 V, the open-circuit voltage (V_{OC}) of the solar cell is at 2.3 eV, as it is dominated by the lower band gap phase separated InGaN. Moreover, a Schottky barrier at the nonoptimal p -GaN–Ni metal contact interface opposes the light-generated current so that the current asymptotically approaches zero prior to the device reaching its V_{OC} ; this Schottky effect is also confirmed through PC1D simulation. Figure 3(b) shows typical light I - V characteristics of solar cells with a semitransparent current spreading layer. In spite of relatively lower short-circuit currents (J_{SC}) due to light absorption by the top current spreading layer, the optimized contacts with p -GaN yield lower series resistance around 30–50 Ω . These solar cells demonstrate V_{OC} 's as high as 2.4 V and fill factors in the 78%–80% range.

The solar cells with semitransparent current spreading layers measure internal quantum efficiencies (IQEs) around 60% at the band edge, as shown in Fig. 4 and external quantum efficiencies around 43%. The major loss mechanisms here are absorption of up to 40% of the incident light by the semitransparent current spreading layer and transmittance of at least 10% of the incident light through the solar cell, as confirmed through spectrometry. Devices with interdigitated grid contacts measure a lower IQE of around 50% at the band edge due to the Schottky barrier at the p -GaN–Ni non-optimized contact and high series resistances. Moreover, this Schottky barrier causes an increase in the cutoff voltage by 0.3 V compared to the devices with semitransparent current spreading layers.

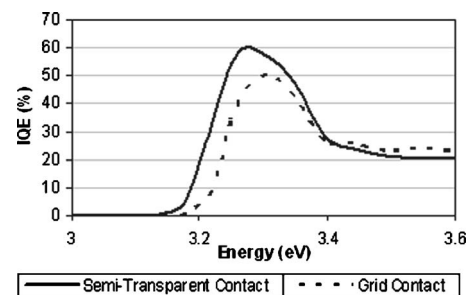


FIG. 4. Internal quantum efficiency curves for two configurations of GaN/InGaN solar cells.

It has been calculated theoretically¹⁵ and measured experimentally¹⁶ that the III-V nitrides are highly pyroelectric materials. The large polarization charge densities present at nitride heterojunction interfaces profoundly influence electric field and mobile carrier distributions, necessitating their incorporation into device design and analysis. Due to high resistivity in such wide band gap semiconductors and challenges in obtaining high *p*-type doping and low-resistance Ohmic contacts, advance structures such as short-period superlattice¹⁷ (SPS) are investigated that involve band gap engineering. SPS structures not only provide better tunneling contacts to *p*-type nitrides but can also be used to increase the lateral conductivity of the device. These topics provide opportunities for further engineering the nitride photovoltaic devices.

In summary, the GaN/InGaN solar cells measure high V_{OC} 's at 2.4 V and consistent IQEs at 60% at their band edge. The primary challenge at the epitaxial growth front of III-V nitride photovoltaics is the reduction of phase separation, as the lower band gap phase-separated material not only reduces the V_{OC} of the solar cell but also enhances recombination decreasing the photogenerated current. The quantum efficiency can be further enhanced by optimizing grid contacts for low Ohmic resistance and be brought close to unity as confirmed through simulations. Presented results are not only a demonstration of InGaN solar cells but also an initial step toward a promising future for III-V nitride photovoltaics. The efficiency of such solar cells can generally be increased by lowering their band gaps and enhancing absorption for practical applications. However, phenomenon such as polarization, which tends to substantially influence the performance of III-V nitride devices, and advance contacting schemes such as short-period superlattices are currently investigated as a next step to enhance III-V nitride solar cell efficiencies. Thus, the III-V nitrides also promise extensive applications in tandems and third-generation ultrahigh efficiency photovoltaics to achieve efficiencies over 50%.

This work was partially funded by DARPA/ARO Agreement No.: W911NF-05-9-0005. This work was also supported by U.S. D.O.E. and the National Renewable Energy

Laboratories, monitored by Dr. Robert McConnell and Dr. Martha Symko-Davies, and the Office of Naval Research, monitored by Dr. Colin Wood.

- ¹S. Nakamura, S. Pearton, and G. Fasol, *The Blue Laser Diode*, 2nd ed. (Springer, Berlin, 2000).
- ²V. Yu. Davydov, A. A. Klochikhin, R. P. Seisyan, V. V. Emtsev, S. V. Ivanov, F. Bechstedt, J. Furthmüller, H. Harima, A. V. Mudryi, J. Aderhold, O. Semchinova, and J. Garul, *Phys. Status Solidi B* **229**, 1 (2002).
- ³J. Wu, W. Walukiewicz, K. M. Yu, J. W. Ager III, E. E. Haller, H. Lu, W. J. Schaff, Y. Saito, and Y. Nanishi, *Appl. Phys. Lett.* **80**, 3967 (2002).
- ⁴T. Matsuoka, H. Okamoto, M. Nakao, H. Harima, and E. Kurimoto, *Appl. Phys. Lett.* **81**, 1246 (2002).
- ⁵M. A. Green, *Proceedings of the Fourth IEEE World Conference on Photovoltaic Energy Conversion*, Waikoloa, USA, 7–12 May 2006 (IEEE, Piscataway, NJ, 2006), p. 15.
- ⁶A. Luque and A. Martí, *Prog. Photovoltaics* **9**, 73 (2001).
- ⁷R. R. King, C. M. Fetzer, K. M. Edmondson, D. C. Law, P. C. Colter, H. L. Cotal, R. A. Sherif, H. Yoon, T. Isshiki, D. D. Krut, G. S. Kinsey, J. H. Ermer, S. Kurtz, T. Moriarty, J. Kiehl, K. Emery, W. K. Metzger, R. K. Ahrenkiel, and N. H. Karam, *Proceedings of the 19th European Photovoltaic Solar Energy Conference*, Paris, France, 7–11 June 2004 (WIP, Munich, Germany and ETA, Florence, Italy, 2004), p. 3587.
- ⁸R. R. King, D. C. Law, C. M. Fetzer, R. A. Sherif, K. M. Edmondson, S. Kurtz, G. S. Kinsey, H. L. Cotal, D. D. Krut, J. H. Ermer, and N. H. Karam, *Proceedings of the 20th European Photovoltaic Solar Energy Conference* Barcelona, Spain, 6–10 June 2005, (WIP, Munich, Germany and ETA, Florence, Italy, 2005), p. 118.
- ⁹A. De Vos, *Endoreversible Thermodynamics of Solar Energy Conversion* (Oxford University Press, Oxford, 1992), p. 90.
- ¹⁰Y. Nanishi, Y. Saito, and T. Yamaguchi, *Jpn. J. Appl. Phys., Part 1* **42**, 2549 (2003).
- ¹¹J. F. Muth, J. H. Lee, I. K. Shmagin, R. M. Kolbas, H. C. Casey, Jr., B. P. Keller, U. K. Mishra, and S. P. DenBaars, *Appl. Phys. Lett.* **71**, 2572 (1997).
- ¹²P. A. Basore and D. A. Clugston, *PC1D Version 5.9*, University of New South Wales, Sydney, Australia, 2003.
- ¹³M. D. Lammert and R. J. Schwartz, *IEEE Trans. Electron Devices* **24**, 337 (1977).
- ¹⁴Y. Huang, O. Jani, E. H. Park, and I. Ferguson, *MRS Symposia Proceedings No. 955E*, edited by C. R. Abernathy, H. Jiang, and J. M. Zavada (MRS, Warrendale, PA, 2007), pp. I07–20.
- ¹⁵V. Fiorentini and F. Bernardini, *Phys. Status Solidi B* **216**, 391 (1999).
- ¹⁶H. Zhang, E. J. Miller, E. T. Yu, C. Poblenz, and J. S. Speck, *Appl. Phys. Lett.* **84**, 4644 (2004).
- ¹⁷M. E. Lin, F. Y. Huang, and H. Morkoç, *Appl. Phys. Lett.* **64**, 2557 (1997).